Nanolime consolidation of the main building stone of the archaeological site of Volubilis (Morocco)

Dalal Badreddine, Kévin Beck, Xavier Brunetaud, Ali Chaaba, Muzahim Al-Mukhtar

Version of Record: https://www.sciencedirect.com/science/article/pii/S129620741930528X
Manuscript_37db7dae77f06065cab5daf91e2abd60

Nanolime consolidation of the main building stone of the archaeological site of Volubilis (Morocco)

Dalal Badreddine[1,2], Kévin Beck[1*], Xavier Brunetaud[1], Ali Chaaba[2], Muzahim Al-Mukhtar[1]

[1] Univ. Orleans, Univ. Tours, INSA-CVL, LaMé – EA7494, 8 rue Léonard de Vinci, F-45072, Orleans, France

[2] University of Moulay Ismail, ENSAM Meknès, Marjane II – Ismailia BP 15290 Al Mansour, Meknès, Morocco

*Corresponding author: Kévin Beck (kevin.beck@univ-orleans.fr)

Abstract

Volubilis is the most important archaeological site in Morocco, considered as a UNESCO world heritage site since 1997. Unfortunately, the sustainability of the site is in danger by the many degradation patterns detected on the site. Urgent interventions are required in order to consolidate and restore the monuments of the site.

In this paper, the efficiency of nanolime as a consolidation treatment for calcarenite stone, the main construction stone of the site, was assessed. To create degraded reference samples, calcarenite samples were subjected to two accelerated aging tests: a thermal shock test and a salt crystallization test. The two tests created damage quite similar to that of the site, namely cracking and surface degradation respectively. These samples were then treated with nanolime according to a protocol defined in relation to the stone properties and the concentration of the product used. After the application of nanolime, the samples were characterized using non-destructive tests (P-wave velocity, capillary absorption, surface hardness, and colorimetric tests) depending on the type of stone damage. On cracked samples, the treatment acted on the surface of the stone while cracks were still present in depth. On salt crystallized samples, the treatment was efficient as it helped recover the lost surface cohesion. Therefore, the nanolime treatment is efficient for stones that are degraded at the surface (sanding, alveolization, scaling) but less so for cracked stones of the Volubilis site.

Keywords: nanolime; consolidation; thermal shock; salt crystallization; calcarenite; Volubilis

1. Introduction

The main objective of this research was to study the efficiency of nanolime as a consolidation treatment of a weathered limestone called calcarenite. Calcarenite is the main building stone of the archeological site of Volubilis, a world heritage site [1] located 30 km north of Meknes city in Morocco (figure 1).

Figure 1: (a) Geographical location of the archeological site of Volubilis, (b) calcarenite stone used as wall rubble and (c) as carved architectural elements

Over the years, exposure to aggressive environmental conditions has caused substantial damage to the site's monuments. The damage has affected the site on two levels: structural disorders that occurred after the Lisbon earthquake in 1755 [2], which caused the collapse of most of the monuments, and disorders that affect the building materials (stones and mortar). According to the ICOMOS glossary-illustrated figures of alterations of the stone [3], the degradation patterns observed in situ can be divided into two categories: biological colonization that alters the aesthetic aspect of the stone and degradation patterns that cause a loss of matter. The latter includes sanding, scaling and alveolization that are due to the crystallization of destructive salts originated in some of the restoration mortars and transported to the stone porosity by water transfer [4], as well as cracking that is caused by climatic variations [5].

Figure 2: Degradation patterns on the site of Volubilis

Even though it is possible to use unweathered calcarenite stones, collected in the quarries close to the site as a replacement to the weathered ones, the replacement would sometimes affect the authenticity of the monuments, especially in the case of carved stones such as the capitals and the columns. Replacement is also unnecessary when the degradation affects only the surface of the stone. In this case, the degraded stones should be treated in situ, using efficient consolidation methods and materials. Consolidation is used to improve the cohesion of weathered stone when decay patterns and cohesion loss are present [6]. Although it is widely used as a conservation practice, it is a risky one due to its non-reversibility and to the possibility of undesirable side-effects. For this reason, before carrying out consolidation work in situ, the efficiency of the consolidation should first be tested through several laboratory studies, the main objectives of which are to ascertain their effectiveness as well as their

potential harmfulness [7]. In these studies, parameters such as stone composition and stone properties, type of consolidation products, application protocols, curing conditions, etc. should be taken into account [7].

In restoration work, consolidants of various kinds are used to recover the initial strength of a damaged stone. Organic consolidants (such as acrylic and epoxy resin and silicone resins), have been widely used and were proved to have mainly good performance of reinforcement and water resistance. That said, there is a reluctance to use this kind of consolidant. Acrylic resin, for example, promotes the growth and spread of bacteria and micro-organisms that can aesthetically alter the stones [8]. Alkoxysilanes (such as methyltrimethoxysilane (MTMOS) and tetraethyl orthosilicate (TEOS)) achieve a good consolidation action due to hydrolysis and condensation reactions that lead to the formation of silica gel inside the pores of the treated stone [9,10]. These silica-based products can penetrate porous materials, but have low chemical compatibility with calcareous substrates and, in some cases, have low efficiency and durability [11]. A dense network of microporous gel that is likely to crack can be formed. This network may obstruct the porosity of the stone by causing a significant reduction in water permeability [12]. Inorganic consolidants are more compatible with calcareous stones [13] from a chemical point of view. This is the case of lime milk which is the result of stirring calcium hydroxide particles $Ca(OH)_2$ in pure water and lime water which is filtered lime milk. However, to achieve a real consolidation with inorganic consolidants, a huge amount of the product is necessary as $Ca(OH)_2$ has very low solubility in water (1.73 g/l at 20°C) [14]. The use of these products causes further damage by transporting soluble salts into the stone that crystallizes during the drying phase of the product. This makes them not only potentially inefficient but could also cause further harm to the stone [15]. Recently, nanolime has been used as a replacement for the incompatible and inefficient consolidants mentioned before. It is a dispersion of calcium hydroxide nanoparticles in alcohols (ethanol, isopropanol, and n-propanol) [16]. When applied to stone, the alcohol evaporates and calcium hydroxide particles are deposited in the porosity of the stone replacing the binder lost in the degraded stone once carbonation is done. Nanolime is a promising consolidation treatment due to his high compatibility with the calcareous substrate. It has also a higher efficiency as it can carry large amounts of lime into the treated substrate (up to 50 g/l), without water [16]. So far, nanolime treatments have been tested on different substrates such as wall paintings, renders, and plasters [17, 18, 19], as well as on highly porous stones like the Maastricht stone and lime-based mortars [20, 21, 22, 23]. For all these reasons, nanolime seems to be a promising consolidation treatment for degraded calcarenite stones. This said, before applying nanolime

to the degraded calcarenite stones of the site of Volubilis, a study was carried out on the treatment of calcarenite, given that it is a very heterogeneous stone with a low porosity of 19% and therefore might require a particular treatment protocol.

2. Research aim

In this study, the efficiency of nanolime as a curative solution for the consolidation of calcarenite stones was assessed. First, unweathered calcarenite samples were artificially degraded and later treated with nanolime. The treated samples were characterized using non-destructive tests (the capillary absorption test, the ultrasonic velocity test, the hardness test, and colorimetric tests) to evaluate the consolidating effectiveness of nanolime.

3. Materials

3.1. Calcarenite stone

Calcarenite stone is the main building stone of the archeological site of Volubilis, representing over 60% of the volume of the site's building stones. It was usually recovered from Ain Schkor quarry, located within 5 km of the site. Calcarenite is a beige-yellowish limestone rich in terrigenous material and large bioclasts [24] containing mostly calcite and quartz [4]. The stone has an average porosity of 19%, close to that of the San Julian calcarenite [25] and lower than other calcarenite like the Maastricht calcarenite (40 to 52% of porosity) [26], the Marsala calcarenite (40 to 60% of porosity) [27] or the Tamala calcarenite (30 to 50% of porosity) [28]. The calcarenite has a bimodal distribution with two distinct pore families: a first principal peak is observed around the pore diameter equal to 20 µm, this type of pores represents the macroporosity, estimated at 52%. The second peak is between 0.1 and 0.3 µm, this type of pores is the mesoporosity of the stone, estimated at less than 27%. The Calcarenite of Volubilis has a capillary coefficient of 2.03 $kg/m^2/h^{0.5}$, and compressive strength of 18.45 MPa. Compared to the previously cited calcarenites, the presently tested calcarenite has a higher compressive strength than the Marsala stone (1.2 to 4 MPa) [27], lower than the san Julian calcarenite (38 MPa) [29]. The Maastricht calcarenite has a wide compressive strength range (5 to 20 MPa) [30]. The presently studied calcarenite in visibly a heterogeneous stone, composed of two distinct parts: a yellow, visibly more porous, part and a white, more compact part (figure 3). Calcarenite has an average ultrasound velocity of 2751 m/s, but due to its apparent heterogeneity, it has an anisotropy index of 15% [31] which indicates that the velocity is higher in a certain direction. The microscopic image of the

calcarenite, taken with a scanning electron microscope Hitachi TM-3000, shows a compact matrix (formed of calcite) surrounding angular quartz grains with a diameter of approximately 100 µm [31].

Figure 3: (a) Calcarenite stone from Ain Schkor quarry (cubic sample 4×4×4 cm^3), (b) microscopic image of the calcarenite (×1000) and (c) pore size distribution of the calcarenite stone

3.2. Nanolime

The product used in this study is a commercial ready to use nanolime CaLoSil E50 (IBZ-Salzchemie GmbH & Co) that became available on the market in 2006. It is a suspension of $Ca(OH)_2$ particles in ethanol with a size range of 50 to 150 nm. CaLoSil E50 carries 50 g of lime per liter, which is approximately 30 times more lime than in traditional limewater.

4. Methods

4.1. Artificial aging test

In order to test the effectiveness of consolidation, nanolime needs to be applied on degraded stones. Calcarenite stone samples were therefore subjected to two artificial aging tests to induce different forms of degradation. For each protocol, three cubic samples (4×4×4 cm^3) of the calcarenite stone, cut from bigger blocks retrieved from the quarry, were tested. The artificial aging procedures used are the following:

- Thermal shock test based on the standard EN 14066 [32]. The test consists of successive cycles of drying at a temperature of 105°C for 24 hours, followed by immediate immersion in water at 20°C. When carried out on the calcarenite stone, the standard normalized aging test had no effect as no visible damage or weight variation was observed [31]. For this reason, and in order to obtain altered samples, we decided to increase the amplitude of temperature variation. The samples were dried at 250°C for 24 hours and then immediately immersed in water at 0°C. The cycles were repeated until the samples were visibly damaged.
- Salt crystallization test carried out according to the standard EN 12370 [33]. All the samples were subjected to successive cycles of immersion for 2 hours in a 14 % solution of $Na_2SO_4,10H_2O$ followed by drying in an oven at 105 °C for 20 hours and cooling at room temperature (20°C) for 2 hours.

4.2. Application protocol of nanolime on the calcarenite stone samples

The application procedure is one of the factors influencing the effectiveness of nanolime. Even though capillary absorption is the most used method of application in laboratory studies, it is not a practical one [6-20-21]. In this study, nanolime was applied by brushing [34] which is commonly adopted in the practice of in-situ conservation [6,7].

To improve the consolidation effect of the treatment, the product is applied more than once. The optimal number of applications ultimately depends on the stone porosity and pore size [35]. Slizkova et al. [21] showed that after the first three applications of CaLoSiL E50 on a highly porous stone such as the Maastricht stone (with an average porosity of 50 %), the water movements became slower, which indicates partial saturation of the pore space. Due to the lower porosity of calcarenite stone (19 %) compared with Maastricht stone, the product was applied three times to the stone [36]. A higher number of applications would not be as effective as $Ca(OH)_2$ particles wound quickly fill the pore space. To define the interval between two consecutive applications, a preliminary test was conducted on a cubic sample of calcarenite stone (4×4×4 cm^3) to determine the time required for the ethanol in the stone sample to dry. Ethanol was applied by brushing to the surface of the stones, that were placed in a controlled environment (20 °C/76 %HR). The drying curve (figure 4), evaluated by measuring the weight loss over time, shows that ethanol was almost entirely evaporated after 90 minutes. The interval between two consecutive applications was defined as 3 hours. All measurements were performed after 28 days of curing [20-37]. During this time, the specimens were placed in a controlled environment, with a temperature of 20°C and relative humidity of 76 %, to enhance the carbonation process and ensure maximum conversion of $Ca(OH)_2$ into $CaCO_3$ [38].

Figure 4: Drying curve of a calcarenite sample treated with ethanol

4.3. Assessment of the effectiveness of the consolidation

The effectiveness of consolidation was assessed using the following non-destructive testing methods:

- P-wave velocity measurements carried out on dried cubic samples (4×4×4 cm^3). It is a non-destructive method that detects any change in the texture of the stone [39]. The test was performed in laboratory conditions (T=20 °C-HR=40 %), using a Pundit Plus apparatus with two piezoelectric transducers with a frequency of 83 kHz.
- Capillary water rise test carried out on dried cubic samples (4×4×4 cm^3), according to the procedure described in the standard NF EN 1925 [40]. The samples were dried at 60°C,

placed in a container where they were immersed in water at a height of 3 ± 1 mm and weighed at regular intervals.

- Hardness test carried out on dried samples. It is a non-destructive test performed using a Piccolo 2 portable hardness tester, in laboratory conditions on cubic samples (4×4×4 cm^3). In each cube, 10 measures were done on each face (at 1 cm intervals) and then averaged to obtain the surface hardness values.
- Colour changes were measured using a Konica spectro-photo-colorimeter. The colour parameters L * a * b *were determined in the CIELab colour space where coordinate L* is the greyscales that correspond to grades of lightness from 0 (black) to 100 (white), a* is the red/green coordinate (negative values represent the green component and positive values represent the red component) and b* is the yellow/blue coordinates (negative values represent the blue component and positive values the yellow one) [41]. With the unweathered stones as a reference, the colour coordinate variation (ΔL*, Δa*, Δb*) was calculated, as well as the total colour variation (ΔE):

$$\Delta E = ((\Delta L^*)^2 + (\Delta a^*)^2 + (\Delta b^*)^2)$$

5. Results and discussion

The two aging tests used in this study damaged the calcarenite stones differently. The thermal shock aging tests induced cracking in the tested samples while the salt crystallization test caused a loss of cohesion and a loss of matter on the surface of the tested samples.

5.1. Nanolime treatment performance for the cracked calcarenite stones

In all the calcarenite stone samples, cracking obtained by thermal shock aging appeared after 2 cycles. On some samples, the cracks were small and present only on one side while for the rest, the cracks were larger and affected two or more faces (figure 5).

Figure 5: Cracked calcarenite stone samples due to thermal shock aging test (4×4×4 cm3)

These samples were treated according to the protocol described in 4.2 and nanolime was applied to the cracked faces of each sample. The samples were weighed before and after each application to determine the quantity of nanolime absorbed as well as the weight variation after 28 days of curing. The nanolime content varied from 0.64 % and up to 1.30 %, depending mainly on the size and depth of the crack present on the treated sample. The wider

and longer the crack is, the more nanolime is absorbed and transported inside the specimens. The samples were placed in a controlled atmosphere (temperature = 20°C and relative humidity = 76 %). When the ethanol evaporates, the carbonation process starts and $CaCO_3$ particles are precipitated inside the cracks, which explains why the weight increased after the treatment for all samples. After 28 days of curing, the weight of samples increased between 0.04% and 0.07%. Then, they were characterized in order to assess the variation in the mechanical and hydraulic properties of the samples, caused by the weathering first and then by the treatment with nanolime.

The predominant method for assessing the effect of aging tests is by measuring the ultrasonic P-wave velocity. The results of the measurements in all three directions of the stone samples are reported in table 1. They were conducted on dried unweathered, weathered and treated samples. Δ_1% represents the variation in the P-wave velocity between the unweathered and weathered samples, and Δ_2% the variation in the P-wave velocity between the treated and non-treated weathered samples (table 1).

The thermal shock test caused a decrease in the ultrasonic P-wave velocity in all three directions of each sample. This decrease indicates that there have been changes in the microstructure with the appearance of cracks that are caused by the difference in the coefficient of expansion of the constituent mineral. These changes cannot be explained considering the bedding of the stone as it could not clearly be identified, not even based on the P-wave velocities measured. Usually, the bedding can be identified when the velocities measured in two directions of stones are similar while the velocity measured in the third direction is higher. In that case, we can assume that the bedding plane is perpendicular to the third direction. This was not the case here, as none of the directions had a velocity that is significantly higher than the two others. Therefore the bedding remains unknown as it does not correspond to any of the principal directions of the stone samples used.

Table 1: Variation in the ultrasonic P-wave velocity after the thermal shock tests and after treatment with nanolime

After the treatment, all specimens showed an increase in the P-wave velocity that varied from 4 to more than 40 %. For all the samples, except sample 1, the increase was greater in the direction where cracks were detected and where the decrease in the P-wave velocity was higher. This means that the cracks allowed a better absorption of the consolidant, and a higher quantity of calcium hydroxide particles was deposited in them after the evaporation of ethanol. The quantity of nanolime absorbed is also related to the size of the cracks. Indeed, the

most damaged sample, sample 3, is the one where the largest cracks appeared, given that the decrease in P-wave velocity in this sample was high. This sample absorbed the highest quantity of nanolime (the weight increased of 1.3%) and had the highest weight variation after 28 days (+0.07%). The cracking of the samples caused a local modification in the porous network, which led to a change (an increase) in the imbibition properties of the stones.

To understand this modification and its effect on the water transfer properties, the capillary imbibition kinetics of the damaged and treated stones was measured and compared to that of the unweathered stones [42]. In fact, the imbibition properties derive directly from the geometry of the porous network (pore size, pore connectivity, etc.) [43]. Figure 6 shows the imbibition capillary curve of the most damaged sample of the three (sample 3) before and after the treatment. These imbibition curves were compared to the imbibition curve of the unweathered sample.

The imbibition curve represents the evolution of the water uptake with the square root of time in the three directions of the cubic stone sample for the weathered sample (black curves) and treated samples (red curves). Compared to the unweathered stone (blue curve), the water uptake of the cracked samples in all three directions is much higher. When the imbibition was done through the cracked surfaces, the samples saturated much more quickly (after 30 minutes) compared to the non-degraded samples where the total saturation took on average 3 hours. Figure 7 shows that water rises faster in the cracks than in the non-cracked parts of the stone. Besides, the water content at the end of the test performed on the weathered sample was almost twice as high as the water content at the end of the test carried out on the unweathered sample.

Figure 6: Capillary imbibition curves of the most damaged sample (sample 3)

Table 2 shows the evolution of the imbibition coefficients in each sample before and after the aging tests and after the treatment with nanolime. It was calculated from the slope of the imbibition curves previously presented. The aging test caused an increase in the imbibition coefficients in all three directions. However, the increase was always smaller in the direction perpendicular to the cracks, in which the decrease in the ultrasound velocity was the highest. In the other directions, the cracks are directly in contact with water, which explains the higher imbibition coefficient.

Table 2: Capillary imbibition coefficients of unweathered, weathered and treated calcarenite stone samples

Figure 7: Capillary imbibition of cracked samples (4×4×4 cm^3)

After treatment, a clear disturbance of the imbibition kinetics was observed. In the directions parallel to the cracks, the imbibition curve of the treated samples could be divided into two distinct parts. If we consider the imbibition curve done through the first direction of sample 3, as shown in figure 6, in the first (Part I), the curve is almost linear and has a much smaller slope than that of the imbibition curve of the unweathered sample, as a result of nanolime treatment and a partial saturation of the pore space with $CaCO_3$ particles. In the second (Part II), the slope of the curve increases drastically and becomes parallel to that of the cracked sample (table 2). However, in the directions perpendicular to the cracks, little to no change in the slope of the imbibition curve between part I and part II was observed given that the non-cracked faces of the sample were not treated.

In the directions parallel to the cracks, the abrupt change in the slope shows that the porous network of the stone was no longer homogeneous. The coefficient of imbibition of the treated part (Part I) was lower than that of the unweathered calcarenite stone. This might indicate that in addition to the cracks, the calcium carbonate particles were also deposited in the pores of the stone, causing a change in the pore space at the surface that was obstructed and consequently slowing the water rise in the sample. However, once the water goes past the treated part, the behavior of the stone is that of the weathered one. Beck [44] observed similar behavior when studying the evolution of the imbibition behavior of an artificially aged tuffeau limestone using the cyclic wetting-drying aging test described previously. The aging caused the appearance of a patina caused by the dissolution of calcium carbonate and its re-crystallization on the evaporation surface of the stone that slowed water movement only at the surface of the samples.

In conclusion, the nanolime treatment does not seal the cracks entirely but it significantly improves the mechanical characteristics of the stone. The P-wave velocity measurements after the treatment prove that the cracks were partially sealed as they were still smaller than those of an unweathered stone. This result is corroborated by the water imbibition curves. The results show that on the surface, the cracks seem to be treated and that the treatment caused the appearance of a patina that slows the imbibition of water at first. Therefore, the beneficial effect is significant but limited to a thin layer at the treated surface while at the core, the hydric and mechanical behavior indicates that the stone is not completely consolidated.

5.2. Nanolime performance in consolidation treatment for salt contaminated calcarenite stones

The salt crystallization protocol caused degradation by the progressive loss of matter on the weathered surface, which is a very common kind of degradation found on the site. The protocol specified by the standard NF 12370 [33] recommends conducting the test for 15 cycles. However, the test was very destructive to the calcarenite stone. At the end of the test, the samples were too damaged to be treated (figure 8).

Figure 8: Damaged calcarenite samples (4×4×4 cm^3) after 15 cycles of the salt crystallization aging test

A second salt crystallization aging protocol was carried that was stopped at the 6th cycle, once visible damage with loss of material started to occur. The average weight variation of the samples during the salt crystallization test is presented in figure 9.

Figure 9: Average weight variation during the first 6 cycles of the salt crystallization aging test [34]

The average dry weight increased at the beginning of the test (during the first three cycles) as a result of the presence of the salt that precipitated in the pores of the tested samples. After that, the weight of the accumulated salt could not be balanced by the lost weight due to loss of surface matter [45], causing a decrease in weight from the fourth cycle on. Unlike the thermal shock protocols, the degradation induced by salt crystallization caused a loss of material. Alveolization was detected on the surface of the stone, resulting from the weathering of the yellow parts by sanding while the white parts remained intact (figure 10). The high percentage of macropores (52%), responsible for the capillary rise phenomenon [46], allowed the stone to absorb high quantities of the saline solution. In addition to that, and according to Zehnder & al. [47], crystallization originates in larger pores (macropores) that are connected to smaller ones (mesopores), causing damage to the stone. This indicates that the macrospores are more concentrated in the yellow parts than in the white parts of the stone, visibly more porous.

Once they were damaged, the treatment was applied to all the damaged faces of the calcarenite samples. The samples were weighed before and after each application to determine the quantity of nanolime absorbed as well as the variation in the dry weight of the specimens.

Figure 10: Calcarenite stone sample (4×4×4 cm^3) (a) before, (b) after the second salt crystallization test and (c) after treatment with nanolime

The nanolime content of the calcarenite immediately after treatment varied between 1.85 and 2.86 %. The high amplitude of the variation in nanolime content can be explained by the heterogeneity of the calcarenite stone. The two parts constituting the stone might have different hydraulic properties, and the amount of nanolime absorbed depends on which part is predominant in the treated sample. After 28 days, the weight variation measured was proportional to the nanolime content, and it was betwwen 0.30% and 0.51%. It is due to the precipitation of calcium hydroxide particles in the porosity of the specimens.

P-wave velocity measurements could not be performed on these degraded samples. The damage occurred mainly at the surface, where there was a loss of cohesion between the grains. Putting the piezoelectric transducers on the samples would have undoubtedly caused further damage, and the contact would not have been ensured due to the eroded surfaces. For these samples, it was possible to quantify the effect of the accelerated aging test, and that of the treatment, with a surface hardness test [48]. The results presented in table 3 show the evolution of the average surface hardness in the samples due to the aging test and to the consolidation treatment.

Table 3: Variation in surface hardness values for the unweathered samples, after the aging test and after nanolime treatment

After the aging test, the stone surface was weakened by the crystallization of Na_2SO_4,H_2O salt. The resulting disintegration of the matrix of the stone caused a decrease in hardness due to the loss of cohesion between the grains. After treatment, an increase in hardness was observed in all the samples, indicating that $CaCO_3$ particles had been deposited on the surface of the stone, replacing the lost materials. The variation in surface hardness after the aging test was the greatest in sample 3, making it the most damaged sample of all three. It was also the sample that absorbed the most nanolime, which helped treat and recover the cohesion loss.

For all three samples, the increase in surface hardness is directly related to the nanolime content of the treated samples. The more nanolime was absorbed, the more $CaCO_3$ was deposited in the stone and the more cohesion recovery was achieved. The treatment with nanolime not only helped recover the loss of surface hardness but also increased it beyond the value of the unweathered stone. The treatment was efficient from a mechanical point of view. However, a change in color was detected on the treated surfaces due to the formation of a white haze.

5.3. Aesthetic compatibility of the treatment by nanolime

The aesthetic aspect of the treatment is an important feature of any restoration work. The aesthetic parameters were studied with a colorimetric test. The results of the colorimetric measurements performed on the thermal shock samples as well as on the salt crystallization samples in table 4.

Table 4: Average colorimetric values of the weathered calcarenite samples before and after nanolime treatment

The thermal shock aging test caused a small change in the aesthetic aspect of the samples, inducing an increase in the L* and a* coordinates and a decrease in the b* coordinate. After the treatment, the samples became slightly whiter and less yellow and the overall color change measured was 3.6. Although the visual appearance of the stone does not affect its durability, it remains an important parameter for the compatibility assessment. Some authors recommend that the color difference ΔE be less than 5 [49-50]. According to this recommendation, the treatment of the cracked stone was compatible.

The salt crystallization aging test caused a decrease in the L* coordinates and an increase in the a* and b* coordinates. This means that the samples were darker, redder and more yellow. After the treatment, an increase in the L* value for all the samples was noticed, which implies a lightening of all the samples that was due to the white haze observed on the surface of the stones, as a part of the nanolime absorbed had actually settled on the surface (figure 10).

When compared to degraded stones, the total color change was 12.19, which is higher than the aesthetic recommended limit. However, when comparing the colorimetric values of the treated stone to that of the unweathered stone, a total change of 4.94 was obtained, which remains within the recommended limit.

6. Conclusion

Nanolime was used as a treatment of calcarenite stone samples degraded in the laboratory using two artificial aging tests to create damage – cracking due to thermal shock and loss of surface degradation due to salt crystallization – similar to the damage observed on the site.

On the cracked stone samples, nanolime proved to be only partially efficient. The treatment caused the formation of a patina induced by the deposition of $CaCO_3$ particles in the pores at the surface. This patina slowed down the water rise during the water imbibition tests but, at the core, the behavior of the treated samples was close to their behavior before nanolime

treatment. Moreover, P-wave velocity measurements of the treated samples were lower than those of an unweathered stone, indicating that at depth the cracks are not completely treated but only sealed partially at the stone surface.

The consolidation of the surface degraded stones with nanolime was efficient as the mechanical properties improved and the surface hardness increased. The replacement of the lost binder of the damaged stone surface by $CaCO_3$ particles induced by the nanolime increased the surface hardness. The increase is directly related to the quantity of nanolime absorbed. The more nanolime was absorbed, the more $CaCO_3$ particles were deposited in the stone and the more cohesion recovery was achieved.

The treatment induced a lightening of the stone samples that was more intense in the salt crystallization samples. However, colorimetric measurements showed that the color change remained within the recommended limits ($\Delta E < 5$) from an aesthetic point of view.

Finally, for the Volubilis site, considering the results of this study, nanolime treatment can be recommended for the stones degraded at the surface (sanding, alveolization, scaling) and to a lesser extent for cracked stones. Another interesting work would be to study the durability and the effectiveness of nanolime, not as a curative solution, but as a preventive treatment to the calcarenite stone.

7. References

[1] UNESCO, Inscription: site archéologique de Volubilis, Maroc. http://whc.unesco.org/archive/1997/whc-97-conf208-17f.pdf, (1997).

[2] Levret A., The effects of the « Lisbon » earthquake in Morocco, Tectonophysics 193 (1–3), 83-94 (1991).

[3] ICOMOS-ISCS, Illustrated glossary on stone deterioration patterns. https://www.icomos.org/publications/monuments_and_sites/15/pdf/Monuments_and_Sites_15_ISCS_Glossary_Stone.pdf (2010).

[4] I. Aalil, K. Beck, X. Brunetaux, K. Cherkaoui, M.A. Chaaba, M. Al-Mukhtar, Deterioration analysis of building calcarenite stone in the House of Venus in the archaeological site of Volubilis (Morocco). Construction and Building Materials, 125, 1127-1141 (2016). https://doi.org/10.1016/j.conbuildmat.2016.09.005

[5] J.M. Vallet, P. Bromblet with the collaboration (in alphabetical order) of R. Bouzidi, A. Daehne, D. Dessandier, M. El Rhoddani, S. Kamel, J. Linke, Guide for the stones conservation of the ancient site of Volubilis (Morocco). Final report, BRGM/RP-58023-FR, 59p (2010).

[6] B. Sena da Fonseca, S. Piçarra, A.P. Ferreira Pinto and M. F. Montemora, Development of formulations based on TEOS-dicarboxylic acids for consolidation of carbonate stones. New Journal of Chemistry 40 (9) (2016). https://doi.org/10.1039/c6nj00455e

[7] J. Delgado Rodrigues, Stone consolidation: research and practice. Int. Symp. On Works of Art and Conservation Science Today (Thessaloniki, Greece) (2010)

[8] F. Hameed, B. Schillinger, A. Rohatsch, M., Zawisky, H. Rauch, Investigations of stone consolidants by neutron imaging. Nuclear Instruments and Methods in Physics Research Section A: Accelerators, Spectrometers, Detectors and Associated Equipment, 605 (1–2) (2009), 150-153. https://doi.org/10.1016/j.nima.2009.01.139

[9] E. Doehne, C. Price, Stone conservation an overview of current research. Getty conservation institute (2010), 159p. https://doi.org/10.2307/3179804

[10] E. Franzoni, G. Graziani, E. Sassoni, TEOS-based treatments for stone consolidation: acceleration of hydrolysis-condensation reactions by poulticing. Journal of Sol-Gel Science and Technology, Volume 74 (2016), 398-405. https://doi.org/10.1007/s10971-014-3610-3

[11] G. Borsoi, B. Lubelli, R. Van Hees, R. Veiga, A. Santos Silva, Understanding the transport of nanolime consolidants within Maastricht limestone. Journal of Cultural Heritage, Volume 18, 242-249 (2016). https://doi.org/10.1016/j.culher.2015.07.014

[12] M.J. Mosquera., D.M. De los Santos, A. Montes, L. Valdez-Castro, New Nanomaterials for Consolidating Stone, 24 (6), (2008), 2772-2778. https://doi.org/10.1021/la703652y

[13] E. Hansen, E. Doehne, J. Fidler, J. Larson, B. Martin, M. Matteini, C. Rodrigues Navarro, E. Sebastian Pardo, C. Price, A. de Tagle, J.M. Teutonico, N. Weiss, A review of selected inorganic consolidants and protective treatment for porous calcareous materials. Studies in Conservation 4, 13-25 (2003). https://doi.org/10.1179/sic.2003.48.Supplement-1.13

[14] C. Rodriguez-Navarro, A. Suzuki, E. Ruiz-Agudo, Alcohol Dispersions of Calcium Hydroxide Nanoparticles for Stone Conservation. Langmuit 29 (2013), 1457-11470. https://doi.org/10.1021/la4017728

[15] G. Borsoi, B. Lubelli, R. Van Hees, R. Veiga, A. Santos Silva, Understanding the transport of nanolime consolidants within Maastricht limestone. Journal of Cultural Heritage, Volume 18, 242-249 (2016). https://doi.org/10.1016/j.culher.2015.07.014

[16] P. D'Armada, E. Hirst, Nanolime for Consolidation of Plaster and Stone. Journal of Architectural Conservation, 18(1) (2012), 63-80 https://doi.org/10.1080/13556207.2012.10785104

[17] J. Vojtěchovský, Surface consolidation of wall paintings using lime nano-suspensions, Acta Polytechnica 57(2) (2017), 139–148 https://doi.org/10.14311/AP.2017.57.0139

[18] G. Borsoi, M. Tavares, R. Veiga, A. Santos Silva, Microstructural characterization of consolidant products for historical renders: an innovative nanostructured lime dispersion and a more traditional

ethyl silicate limewater solution**.** Microscopy and Microanalysis 18(5) (2012), 1181-1189 https://doi.org/10.1017/S1431927612001341

[19] R. Giorgi, L. Dei, P. Baglioni, A new method for consolidating wall paintings based on dispersions of lime in alcohol. Studies in conservation, 45(3) (2000), 154-161 https://doi.org/10.1179/sic.2000.45.3.154

[20] G. Borsoi, B. Lubelli, R. Van Hees, R. Veiga, A. Santos Silva, Application protocol for the consolidation of calcareous substrates by the use of nanolimes: From Laboratory Research to practice**.** Restoration of Buildings and Monuments, 22(4-6) (2017), 99–109 https://doi.org/10.1515/rbm-2016-0008

[21] Z. Slizkova, D. Frankeova, Consolidation of porous limestone with nanolime, laboratory study. 12th International Congress on the Deterioration and Conservation of stone (Columbia University, New York) (2012)

[22] A. Daehne, C. Herm, Calcium hydroxide nanosols for the consolidation of porous building materials – results from EU-STONECORE. Heritage Science 1(1) (2013), 1-11 https://doi.org/10.1186/2050-7445-1-11

[23] J. Otero, V. Starinieri, A.E. Charola, Nanolime for the consolidation of lime mortars: A comparison of three available products. Construction and building materials, 181 (2018), 394-407 https://doi.org/10.1016/j.conbuildmat.2018.06.055

[24] D. Dessandier with the collaboration of F. Antonelli, R. Bouzidi, M. El Rhoddani, S. Kamel, L. Lazzarini, L. Leroux, M. Varti-matarangas, Atlas of the ornamental and building stones of Volubilis ancient site (Morocco). Final report, BRGM/RP-55539-FR (2008), 166p.

[25] V. Brotons, R. Tomàs, S. Ivorra, J.C. Alarcon, Temperature influence on the physical and mechanical properties of a porous rock: San Julian's calcarenite. Engineering Geology 167 (2013), 117-127 (2013) https://doi.org/10.1016/j.enggeo.2013.10.012

[26] D.J.M. Ngan-Tillard, W. Verwaal, A. Mulder, H.K. Engin, R. Ulusay, Application of the needle penetration test to a calcarenite, Maastricht, the Netherlands. Engineering Geology 123 (2011), 214-224. https://doi.org/10.1016/j.enggeo.2011.08.004

[27] M. Zimbardo, L. Ercoli, C. Cannone, A. Nocilla, The safety of an industrial archaeological heritage: The underground quarries in Marsala (Sicily). Geotechnical Engineering for the Preservation of Monuments and Historical Sites, Taylor & Francis Group, London, Editors: Bilotta, Flora, Lirer & Viggian (2013), 785-792. https://doi.org/10.1201/b14895-91

[28] A. Smith, S. Massuel, D. Pollock, P. Dillon, Geohydrology of the Tamala Limestone Formation in the Perth Region: Origin and role of secondary porosity, CSIRO: Water for a Healthy Country National Research Flagship (2011), 63 pp. https://doi.org/10.4225/08/599dd0fd98a44

[29] V. Brotóns, S. Ivorra, J. Martínez-Martínez, R. Tomás, D. Benavente, Study of creep behavior of a calcarenite: San Julián's stone Alicante. Materiales de Construcción 63 (2013), 581-595. https://doi.org/ 10.3989/mc.2013.06412

[30] C.W. Dubelaar, M. Dusar, R. Dreesen, W.M. Felder, T.G. Nijland, Maastricht limestone: a regionally significant building stone in Belgium and The Netherlands. Extremely weak, yet time resistant. Heritage, Weathering and Conservation 2, Taylor and Francis Group (2006), 9–14.

[31] I. Aalil, Contribution to the study of the built heritage: methods of diagnosis of the pathologies of structures and means of restoration. Case study: Archeological site Volubilis in Morocco. PhD thesis, University of Orleans (France) and University Moulay Ismail (Morocco) (2017), 172p.

[32] Standard EN 14066, Natural stone test methods – Determination of resistance to ageing by thermal shock, 10p (2013)

[33] Standard EN 12370, Natural stone test methods - Determination of resistance to salt crystallization, 7p (1999)

[34] D. Badreddine, K. Beck, X. Brunetaud, A. Chaaba, M. Al-Mukhtar; Study of effectiveness of treatment by nanolime of the altered calcarenite stones of the archeological site of volubilis site (Morocco). 7th International Conference, EuroMed (2018), 248-258. https://doi.org/10.1007/978-3-030-01762-0_21

[35] C. Rodriguez-Navarro and E. Ruiz-Agudo, Nanolimes: from synthesis to application. Pure and Applied Chemistry, Vol 90 (3) (2017) https://doi.org/10.1515/pac-2017-0506

[36] G. Taglieri, J. Otero, V. Daniele, G. Gioia, L. Macera, V. Starinieri, A.E. Charola, The biocalcarenite stone of Agrigento (Italy): Preliminary investigations of compatible nanolime treatments. Journal of Cultural Heritage, 30 (2018), 92-99 https://doi.org/10.1016/j.culher.2017.11.003

[37] S.A. Ruffolo, M.F. La Russa, P. Aloise, C.M. Belfiore, A. Macchia, A. Pezzino, G.M. Crisci, Efficacy of nanolime in restoration procedures of salt weathered limestone rock. Applied Physics A, 114 (3) (2014), 753–758. https://doi.org/10.1007/s00339-013-7982-y

[38] J. Otero, A.E. Charola, C.A. Grissom, V. Starinieri, An overview of nanolime as a consolidation method for calcareous substrates, Ge-conservacion 11 (2017), 71-78.

[39] J. Martinez-Martinez, D. Benavente, M.A. Garcia del Cura, Spatial attenuation: the most sensitive ultrasonic parameter for detecting petrographic features and decay processes in carbonate rocks. Engineering Geology 119 (3-4) (2011), 84-95 https://doi.org/10.1016/j.enggeo.2011.02.002

[40] Standard EN 1925, Determination of the water absorption coefficient by capillarity, 10p (1999)

[41] K. Beck, S. Janvier-Badosa, X. Brunetaud, Akos Török, M. Al-Mukhtar, Non-destructive diagnosis by colorimetry of building stone subjected to high temperatures. European Journal of Environmental and Civil Engineering, 20 (6) (2016), 643-655 https://doi.org/10.1080/19648189.2015.1035804

[42] V. Daniele, G. Taglieri,, Nanolime suspensions applied on natural lithotypes: The influence of concentration and residual water content on carbonatation process and on treatment effectiveness. Journal of Cultural Heritage, 11(1) (2010), 102–106. https://doi.org/10.1016/j.culher.2009.04.001

[43] K. Beck, Étude des propriétés hydriques et des mécanismes d'altération des pierres calcaires à forte porosité. PhD Thesis, University of Orléans, 226p (2006)

[44] K. Beck and M. Al-Mukhtar, Cyclic wetting-drying ageing test and patina formation on tuffeau limestone**.** Environmental Earth Sciences, 71 (5) (2014), 2361-2372 https://doi.org/10.1007/s12665-013-2637-z

[45] M. Angeli, J.P. Bigas, D. Benavente, B. Menéndez, R. Hébert, C. David, Salt crystallization in pores: quantification and estimation of damage**.** Environmental Geology, SpringerVerlag New York, 52 (2) (2007), 187-195 https://doi.org/10.1007/s00254-006-0474-z

[46] P. Croveri, D. Luigi, C. Joann, O. Chiantore, Porosimetric changes and consequences for damage phenomena induced by organic and inorganic consolidation treatments on highly porous limestone. Science and Art: A Future for Stone, Proceedings of the 13th International Congress on the Deterioration and Conservation of Stone 1 (2016), 67–74.

[47] K. Zehnder, and A. Arnold, Crystal growth in salt efflorescence. Journal of Crystal Growth 97 (1989), 513–521. https://doi.org/10.1016/0022-0248(89)90234-0

[48] H. Viles, A. Goudie, S. Grab, J. Lalley, The use of the Schmidt Hammer and Equotip for rock hardness assessment in geomorphology and heritage scienc : A comparative analysis. Earth surface processes and landforms, 36 (3) (2011). https://doi.org/10.1002/esp.2040

[49] H.S. Sasse, R. Snethlage, Methods for the evaluation of stone conservation treatments. Saving Our Architectural Heritage: The Conservation of Historic Stone Structures (1997), 223-243

[50] J. Delgado Rodrigues, A. Grossi, Indicators and ratings for the compatibility assessment of conservation actions. Journal of Cultural Heritage 8(1) (2007), 32-43 https://doi.org/10.1016/j.culher.2006.04.007


Rabat
الرباط
Fès
فاس
Meknès
مكناس
Casablanca
الدار البيضاء
Marrakech
مراكش
Maroc

(a)

(b)

(c)

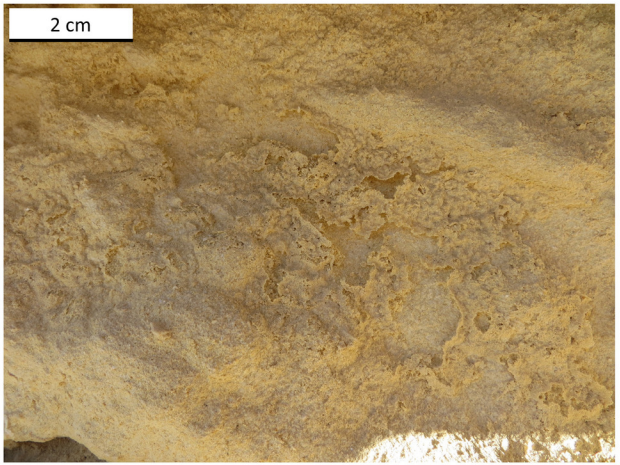

Sanding

Alveolization

Scaling

Cracking

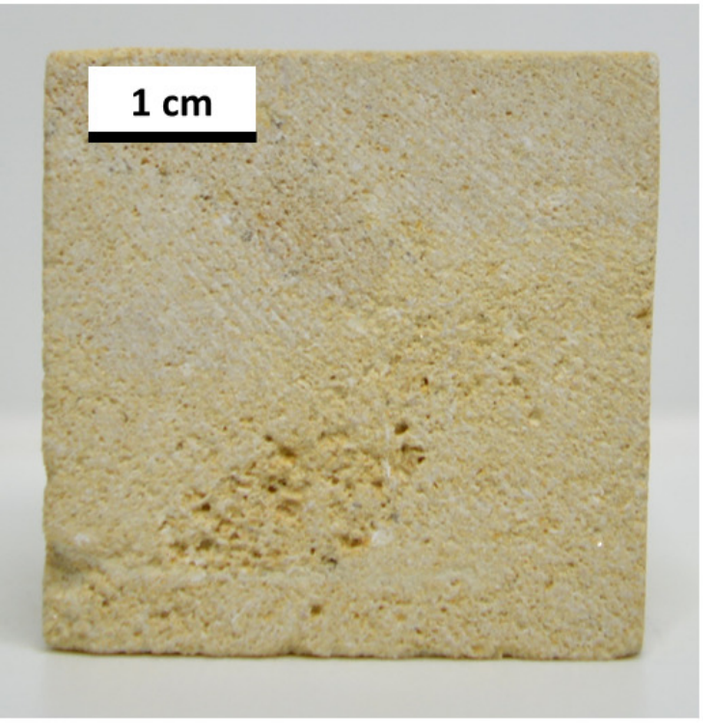
1 cm

(a)

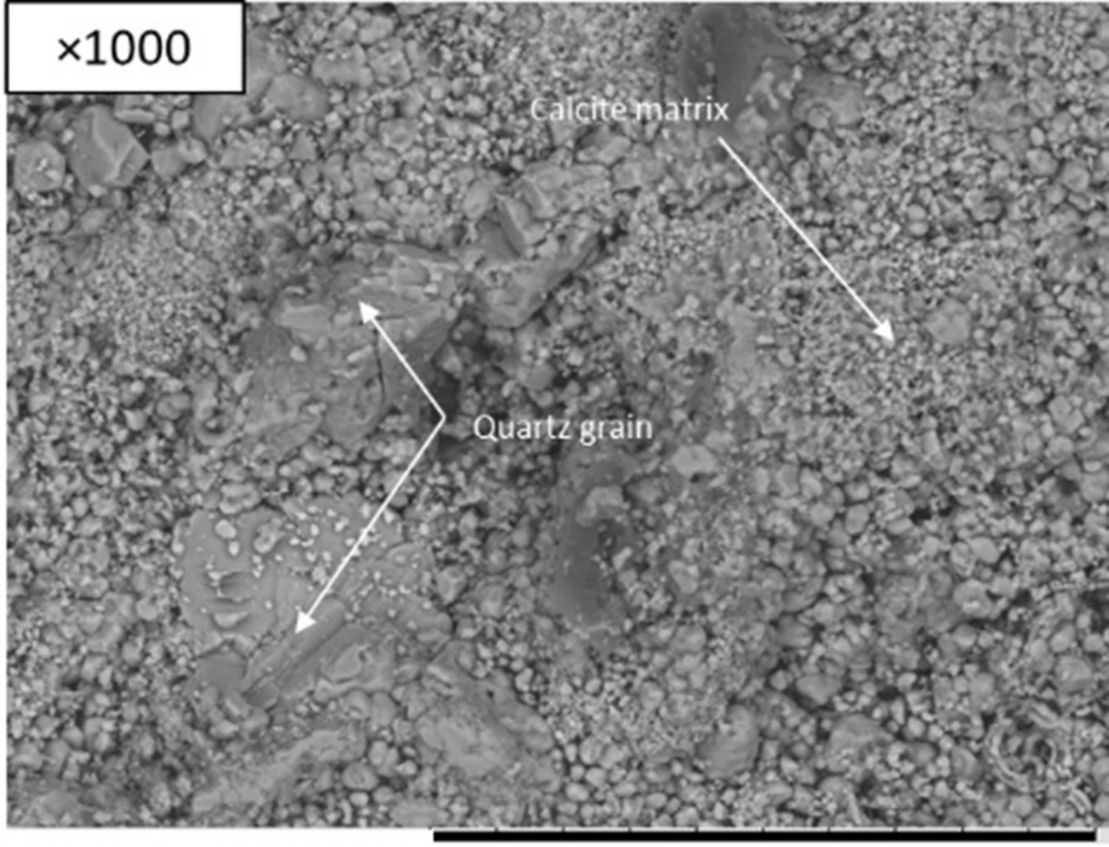
×1000
Calcite matrix
Quartz grain
100 µm

(b)

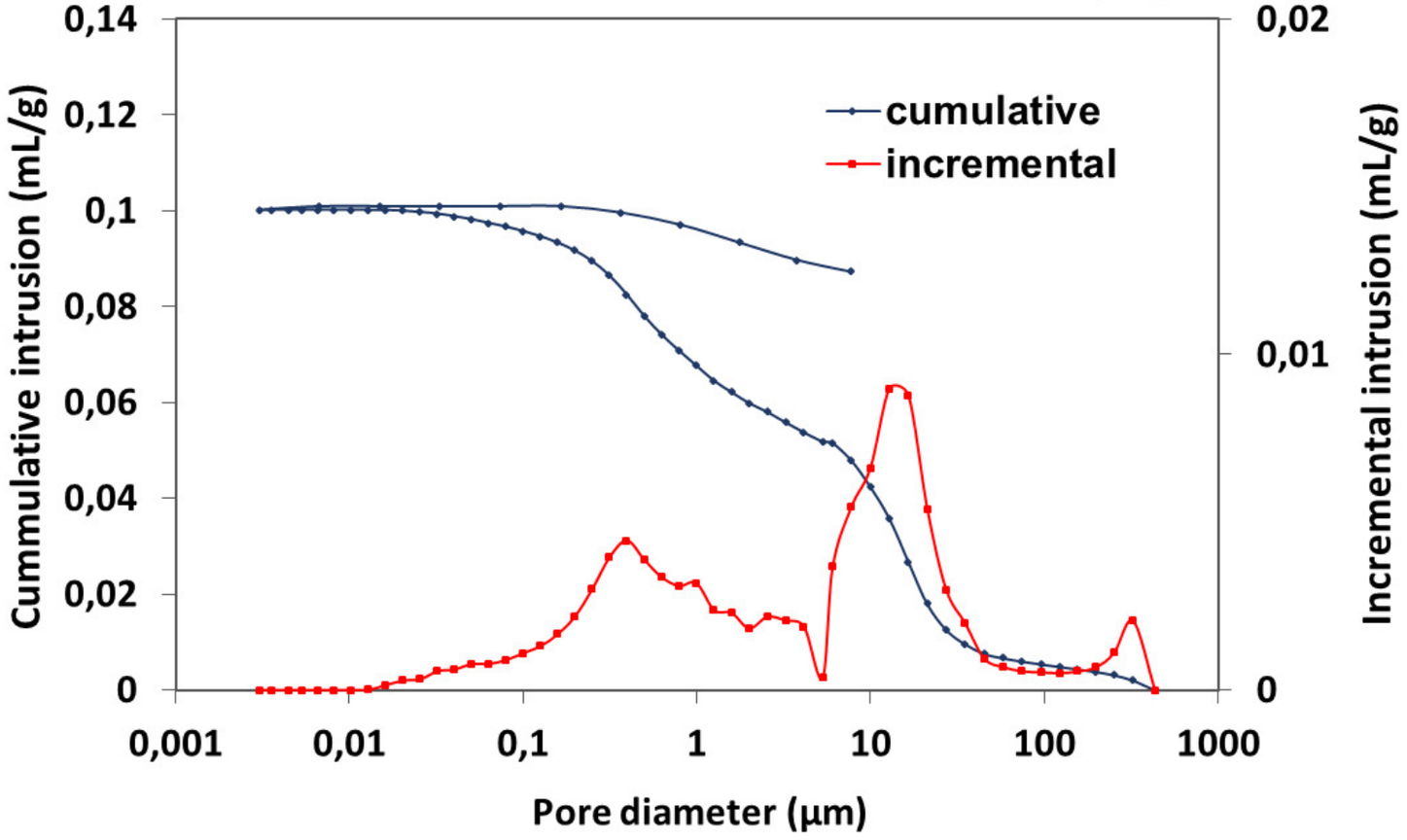
0,14
0,12
0,1
0,08
0,06
0,04
0,02
0
Cummulative intrusion (mL/g)
0,02
0,01
0
Incremental intrusion (mL/g)
cumulative
incremental
0,001
0,01
0,1
1
10
100
1000
Pore diameter (µm)

(c)

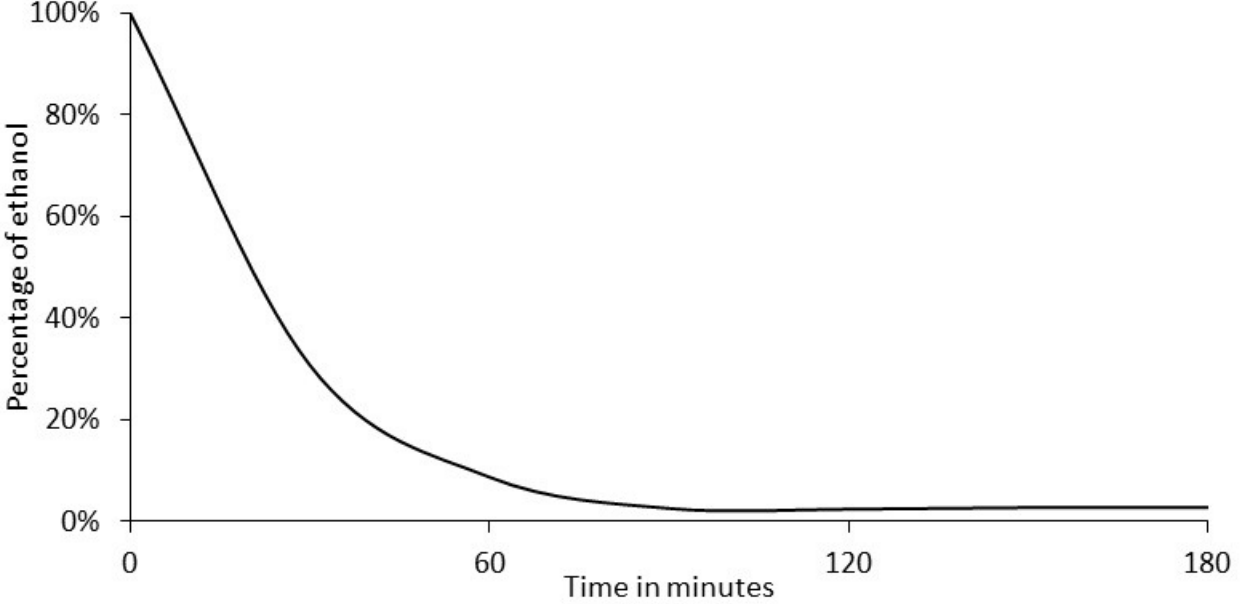
100%
80%
60%
40%
20%
0%
Percentage of ethanol
0
60
120
180
Time in minutes

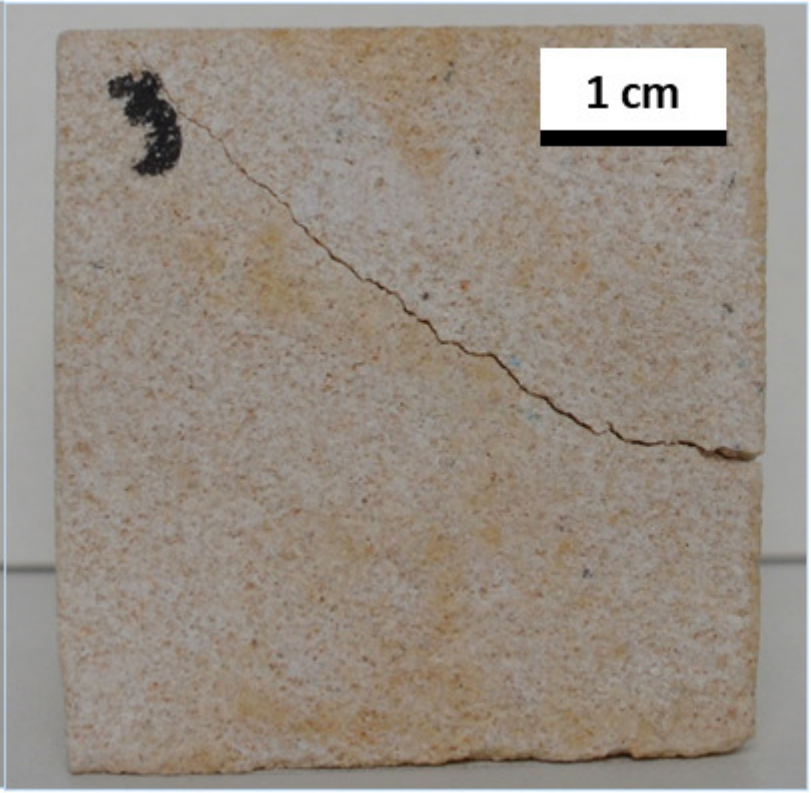
1 cm

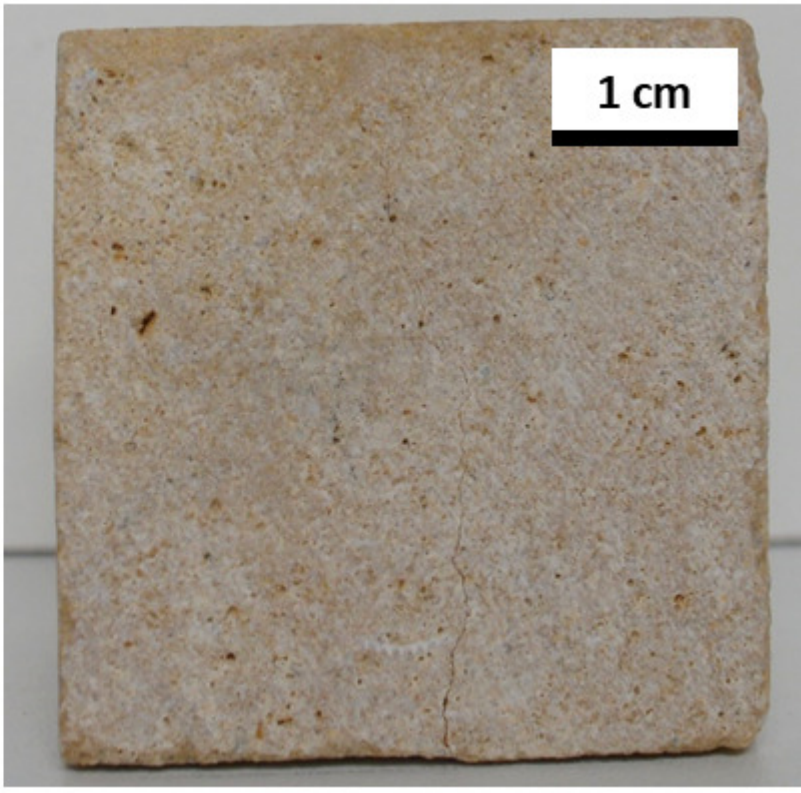
1 cm

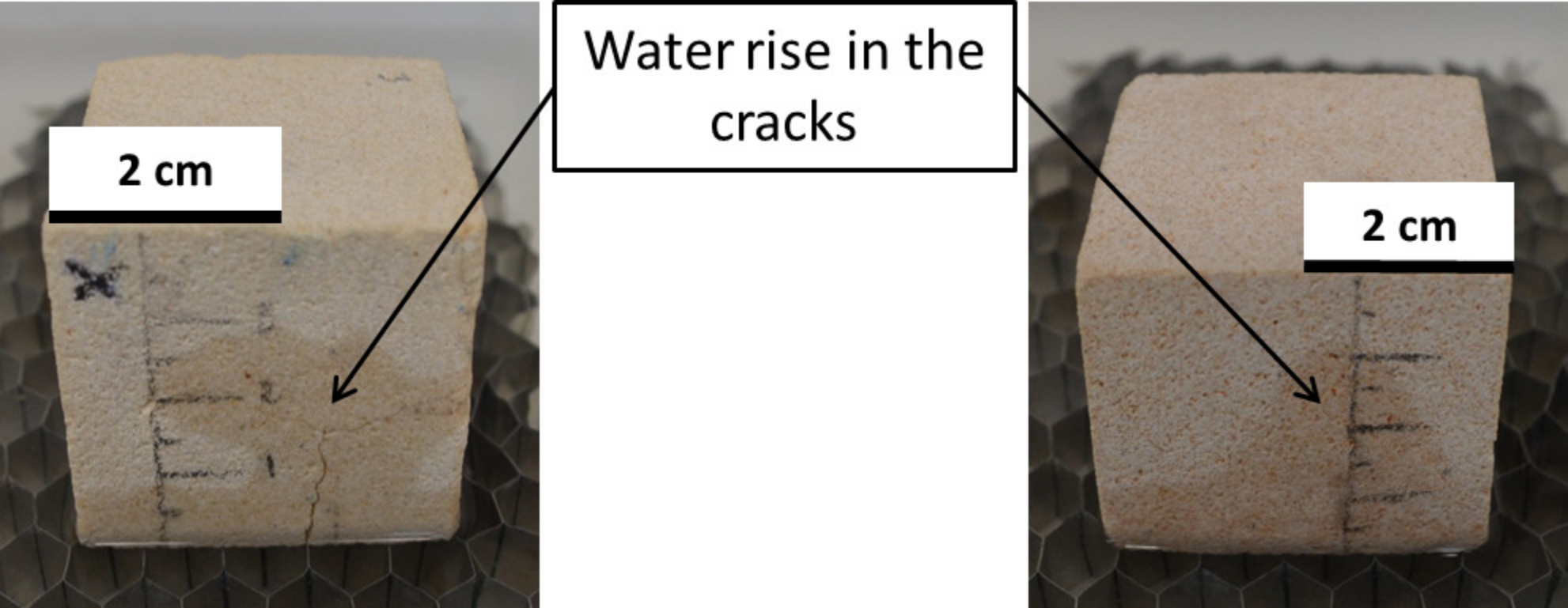
Water rise in the cracks
2 cm
2 cm

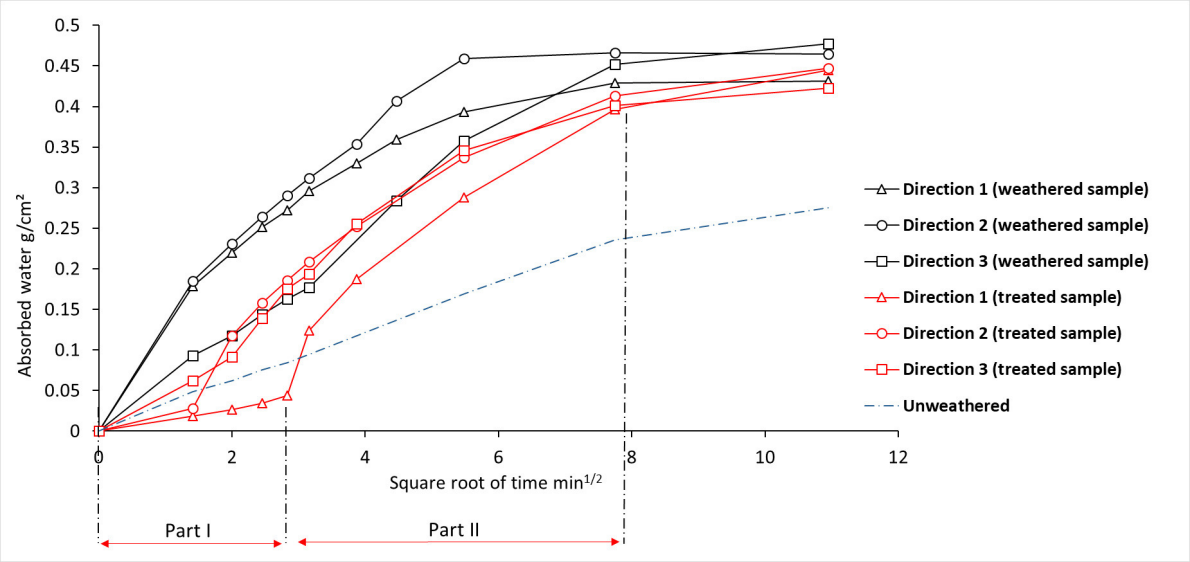
0.5
0.45
0.4
0.35
0.3
0.25
0.2
0.15
0.1
0.05
0
Absorbed water g/cm²
0
2
4
6
8
10
12
Square root of time min1/2
Part I
Part II
Direction 1 (weathered sample)
Direction 2 (weathered sample)
Direction 3 (weathered sample)
Direction 1 (treated sample)
Direction 2 (treated sample)
Direction 3 (treated sample)
Unweathered


2 cm

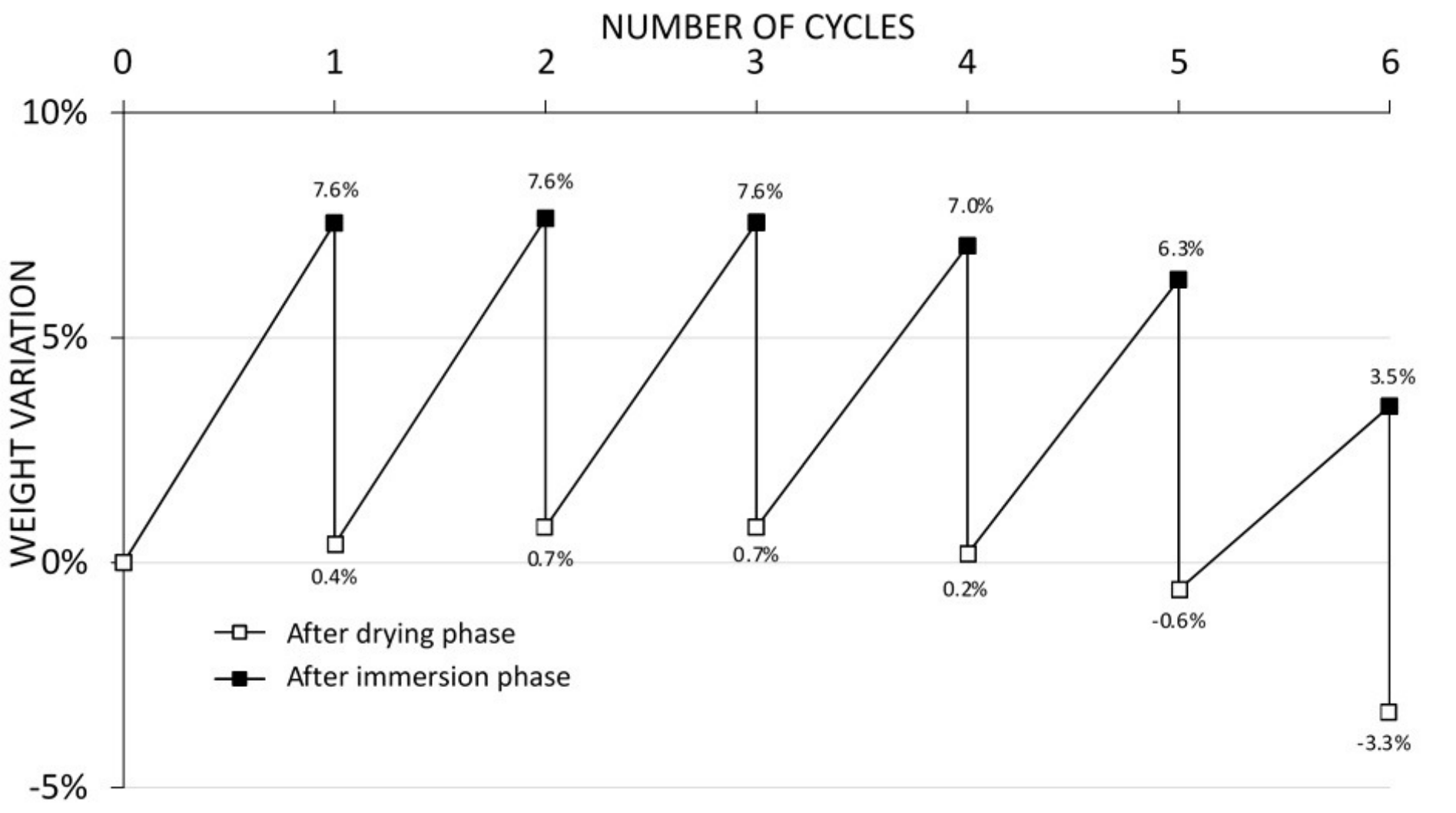
NUMBER OF CYCLES
0
1
2
3
4
5
6
10%
5%
0%
-5%
WEIGHT VARIATION
7.6%
7.6%
7.6%
7.0%
6.3%
3.5%
0.4%
0.7%
0.7%
0.2%
-0.6%
-3.3%
After drying phase
After immersion phase

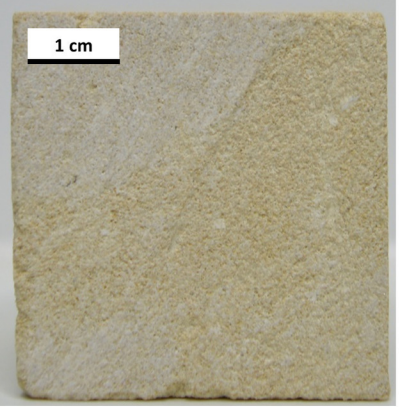

(a)

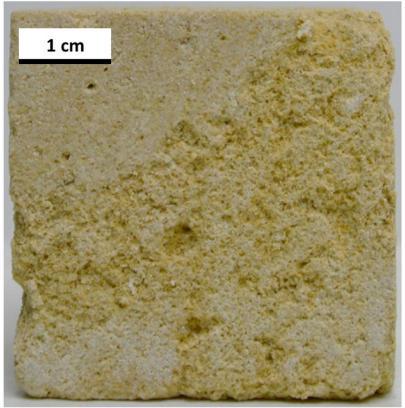

(b)

(c)

Table 1: Variation in the ultrasonic P-wave velocity after the thermal shock tests and after treatment with nanolime

Thermal shock		**Unweathered samples (m/s)**	**Weathered samples (m/s)**	**Δ_1%**	**Treated samples (m/s)**	**Δ_2%**
Sample 1	Direction 1	1990	1626	-18%	2341	+44%
	Direction 2	2797	1389	-50%	1528	+10%
	Direction 3	3175	2105	-34%	2463	+17%
Sample 2	Direction 1	2360	1854	-21%	1928	+4%
	Direction 2	2857	2260	-21%	2418	+7%
	Direction 3	3150	1869	-41%	2654	+42%
Sample 3	Direction 1	2339	1581	-32%	1644	+4%
	Direction 2	2439	1970	-19%	2285	+16%
	Direction 3	3140	1377	-56%	2010	+46%

Table 2: Capillary imbibition coefficients of unweathered, weathered and treated calcarenite stone samples

		Unweathered ($g/cm^2/min^{1/2}$)	Weathered ($g/cm^2/min^{1/2}$)	Treated ($g/cm^2/min^{1/2}$)	
Sample 1	// to the crack (Direction 3)	0.026 ± 0.002	0.049 (+88%)	Part I	0.019 (-26%)
				Part II	0.047 (+80%)
	// to the crack (Direction 1)		0.045 (+73%)	Part I	0.020 (-23%)
				Part II	0.043 (+65%)
	⊥ to the crack (Direction 2)		0.039 (+50%)	Part I	0.038 (+46%)
				Part II	0.041 (+57%)
Sample 2	// to the crack (Direction 3)	0.020 ± 0.001	0.054 (+170%)	Part I	0.012 (-40%)
				Part II	0.026 (+30%)
	// to the crack (Direction 1)		0.055 (+175%)	Part I	0.014 (-30%)
				Part II	0.045 (+125%)
	⊥ to the crack (Direction 2)		0.048 (+140%)	Part I	0.042 (+110%)
				Part II	0.046 (+130%)
Sample 3	// to the crack (Direction 3)	0.027 ± 0.002	0.067 (+148%)	Part I	0.016 (-40%)
				Part II	0.071 (+162%)
	// to the crack (Direction 1)		0.073 (+170%)	Part I	0.015 (-40%)
				Part II	0.069 (+155%)
	⊥ to the crack (Direction 2)		0.048 (+78%)	Part I	0.041 (+50%)
				Part II	0.053 (+96%)

Table 3: Variation in surface hardness values for the unweathered samples, after aging test and after nanolime treatment

	Unweathered samples	**Damaged samples**	**Loss of surface cohesion**	**Treated samples**	**Surface cohesion recovery**
Sample 1	420 ± 26	406 ± 22	-3 %	417 ± 18	3 %
Sample 2	401 ± 23	389 ± 25	-3 %	427 ± 11	10 %
Sample 3	309 ± 29	280 ± 35	-9 %	317 ± 15	13 %

Table 4: Average colorimetric values of the weathered calcarenite samples before and after nanolime treatment

Thermal shock protocol	**Colorimetric values**	**Cracked sample**	**Treated samples**	**Δ%**		
	L*	80.62 ± 0.40	82.44 ± 1.01	2%		
	a*	2.56 ± 0.09	2.91 ± 0.26	14%		
	b*	12.48 ± 0.37	9.35 ± 0.11	-25%		
	ΔE	3.6				
Salt crystallization protocol	**Colorimetric values**	**Unweathered samples**	**Salt-Damaged samples**	**Δ%**	**Treated samples**	**Δ%**
	L*	82.04 ± 0.31	73.65 ± 0.35	-10%	80.18 ± 0.06	9%
	a*	3.17 ± 0.12	4.56 ± 0.27	44%	2.76 ± 0.03	-39%
	b*	13.60 ± 0.96	19.18 ± 1.01	41%	9.04 ± 1.37	-53%
	ΔE		10.17		12.19	
	ΔE (compared to the unweathered stone)				4.94	